Influence of Organic Matrix on the Post-Mortem Destruction of Molluscan Shells
Author(s): Clare P. Glover and Susan M. Kidwell
Source: *The Journal of Geology*, Vol. 101, No. 6 (Nov., 1993), pp. 729-747
Published by: The University of Chicago Press
Stable URL: http://www.jstor.org/stable/30065153
Accessed: 20-09-2016 16:15 UTC

Influence of Organic Matrix on the Post-Mortem Destruction of Molluscan Shells[1]

Clare P. Glover[2] *and Susan M. Kidwell*
Department of Geophysical Sciences,
University of Chicago, 5734 S. Ellis Avenue, Chicago IL 60637 USA

ABSTRACT

To examine the role of organic constituents in the destruction of calcium carbonate skeletons, we aged fresh shells of the bivalves *Nucula sulcata* (organic-rich nacreous aragonites with low crystallite surface areas) and *Cerastoderma edule* (organic-poor porcellaneous aragonites, high crystallite surface areas) under both sterile and non-sterile ("microbial") conditions in aragonite-undersaturated, -saturated, and -supersaturated seawaters for periods up to 11 months. Deterioration was tracked by SEM and weight-loss, and compared to damage produced by reagents of specific effect. The same qualitative sequence of damage was observed in all tanks for both species, but rates of deterioration were $\geq 2\times$ higher in microbial than in sterile tanks at a given saturation state, and were as high or higher in the microbial saturated and supersaturated tanks than in the sterile *under*saturated tank. Damage to shell surfaces was limited almost entirely to loss of organic matrix, which eventually exposed and loosened surficial crystallites. Mineral dissolution in undersaturated tanks was apparently limited to crystallites occurring as loose particulate matter, as direct pitting of shell surfaces was rare. Shells of organic-rich aragonites did not suffer greater weight loss than those with organic-poor aragonites, but in microbial tanks they did suffer more rapid and intense microboring. The only macroscopic evidence of microstructural deterioration was a loss of surface sheen. The experiments show that intraskeletal matrix plays a more complex role in the persistence of calcium carbonate shells than generally appreciated, and that the dynamics of dissolution for fresh biogenic carbonates may differ significantly from the behavior of aged or organic-free carbonate grains used in most laboratory studies. Organics initially protect crystallites (evidenced by slow shell deterioration in sterile tanks): this may counterbalance the effects of undersaturated water and high crystallite surface areas for at least the first several months of aging. With progressive breakdown, however, organics increase shell vulnerability to crystallite-by-crystallite disintegration and, as a microbial substrate, appear to fuel dissolution and microboring. Organic-rich microstructures thus may ultimately have lower preservation potential than organic-poor types. Only after intercrystalline organics have been lost should shell destruction be dominated by mineralogy, microstructural surface area, and ion adsorption. The initial period of low mineral reactivity in fresh shells may help to explain why in situ sediments show lower dissolution rates than expected from laboratory measurements. The experiments also suggest that no aerobic environment should be considered as taphonomically or diagenetically neutral, since matrix decomposes in supersaturated waters and even under sterile conditions, albeit slowly. This overall vulnerability of organic-rich microstructures suggests the potential for systematic biases in the taxonomic and age-class composition of fossil datasets, since ecological groups and evolutionary lineages differ in their shells' microstructures, and since the proportion of organics within carbonate skeletons may vary both with latitude and through individual ontogeny.

Introduction

The reactivity of biogenic carbonates is determined in part by differences in the mineralogy, surface area, and ion adsorption of constituent crystallites (Keir 1980; Walter and Morse 1984, 1985; Walter 1985; Morse 1986; Flessa and Brown 1983; Smith et al. 1992). Many geochemists believe that the organic matrix in which crystallites are embedded is probably also important (review by Morse 1986). However, the relative importance of mineral and organic constituents in different early diagenetic environments and how these roles change during post-mortem aging remains uncertain. Such

[1] Manuscript received September 1, 1992; accepted March 18, 1993.

[2] Current address: Department of Geology and Geophysics, University of Edinburgh, Grant Institute, West Mains Road, Edinburgh EH9 3JW U.K. Reprint requests to SMK.

[The Journal of Geology, 1993, volume 101, p. 729–747] 0022-1376/93/10106-002$1.00

information would be useful not only geochemically but also paleobiologically, because intraskeletal organics are common to all skeletonized groups and vary in content among higher taxa and life habits. Organically mediated disintegration of carbonates occurs in a variety of temperate environments (references below) but has not been quantified and is commonly ignored in discussions of carbonate cycling and fossil preservation. Intraskeletal organics have received slight attention, probably in part because they are a minor shell component by weight (e.g., range of 0.01 to 5% across bivalve microstructures; Hare and Abelson 1965) and because matrix composition, particularly the insoluble framework components that usually predominate, is still poorly known for some important groups (e.g., foraminifera, radiolarians, coccolithophorids; Lowenstam and Weiner 1989). Organics are nonetheless an integral component of skeletal microstructures and are intimately associated with the mineral phase, serving in life both as a template for biomineralization (Lowenstam and Weiner 1989) and as an elastic, strength-enhancing mortar (Currey 1990).

A variety of post-mortem roles, not mutually exclusive, has been suggested for organic matrix: (1) as a binder that, upon leaching or decomposition, releases crystallites and accelerates physical disintegration (Alexandersson 1975, 1978; Lewy 1975, 1981; Emig 1990; Simon et al. 1990); (2) as a coating that protects crystallites from ambient waters and thus inhibits dissolution (Kennedy and Hall 1967; Heinrich and Wefer 1986); (3) as a fuel for bioeroders, which actively destroy shell and whose respiration might also cause local dissolution (Jensen and Thomsen 1987; Roux et al. 1989; Gaspard 1989; Simon and Poulicek 1990); and (4) as a substratum for chemical reactions that produce more stable minerals (Turekian and Armstrong 1961; Pilkey and Goodell 1964; Gaspard 1989). Previous work has varied greatly in the types of carbonate grains studied and in their condition at the start of the experiment, in the aeration, microbial activity and salinity of the experimental waters and whether the saturation state is known, and in the sampling intervals and metrics for microstructural deterioration.

To explore the effects of organic matrix on the reactivity of biogenic carbonates, we tracked the deterioration of bivalve shells in artificial seawaters maintained at three qualitatively different but realistic saturation states (within the natural seawater range of pH ~ 7.8 to 8.2). To distinguish the effects of matrix and mineral reactivity and also the relative effectiveness of biotic and abiotic processes in shell deterioration, each saturation state was run under both sterile (mercuric) and nonsterile conditions (microbes present), and each tank contained shells composed of both organic-rich (nacreous) and organic-poor (porcellaneous) aragonitic microstructures. Shells were taken directly from live populations and, other than having soft tissues removed, were not treated in any way before being placed in experimental tanks. The experiments produced time-series data based on SEM and cumulative weight-loss for periods up to 11 months.

Methods

Water Chemistry. Artificial seawater (ASW) was mixed after the method of Kester et al. (1967) with relative proportions of ions revised to the more recent natural seawater determination of Drever (1982). Only the top 12 major ions were added (Cl^-, Na^+, SO_4^{--}, Mg^{++}, Ca^{++}, K^+, Br^-, Sr^{++}, B, F^-, PO_4^{--}, Fe). Atomic adsorption spectrophotometry was used to verify their concentrations at the start of the experiment and to verify the concentrations of Ca^{++} and Na^+ after 3 and 4 months. Orthophosphate was sufficiently low ($\leq$0.14 ppm) that it should not have poisoned aragonite dissolution (Walter and Burton 1986). ASW is capable of supporting bacterial growth (Kester et al. 1967; lab verification).

Three liters of ASW were added to each of six acid-washed glass containers, which were covered with loosely fitting plastic sheets. Three tanks designated as "microbial" were inoculated with 10 ml of liquid from clam flesh allowed to decompose 1 day in room temperature ASW, and 10 ml of phosphate-free liquid invertebrate food as an additional microbial substrate. Three tanks designated "sterile" were poisoned with sufficient $HgCl_2$ to create a 10 ppm mercuric environment, a common protocol in treating live samples for C-isotope work. Microbial activity was not verified independently, but the appearance of microborings in shells from each of the microbial tanks and the complete lack of microborings in shells from sterile tanks provides a qualitative, post-hoc verification. Tanks were maintained at room temperature (25 $\pm$ 3°C) for the duration of the experiment. To aerate and keep waters comparably mixed, each tank was fitted with an identical micropore bubbler, which was positioned at the center of the tank floor. These introduced laboratory air at a rate of 25 ml/minute. Tanks were also stirred gently once a day during pH measurement.

The pH was adjusted to produce qualitatively

different levels of aragonite undersaturation (Ω_{arag} = 0.5, pH 7.83), saturation (Ω_{arag} = 1.0, pH 7.98), and supersaturation ($\Omega^{arag} \geq 1.5$, pH $\geq$ 8.13) by addition of 1M HCl. The target pH for these states were calculated using the equation

$$a_{H^+} = \sqrt{\frac{m_{Ca^{++}} K'_H K'_1 K'_2 P_{CO_2}}{K'_{arag} \Omega_{arag}}},$$

where $K'_H = 2.8405 \times 10^{-2}$ (Weiss 1974), $K'_1 = 1.00 \times 10^{-6}$ (Mehrbach et al. 1973), $K'_2 = 0.767 \times 10^{-9}$ (Mehrbach et al. 1973), and $K'_{arag} = 6.65 \times 10^{-7}$ mol^2kg^{-1} (Morse et al. 1980). mCa^{++} at the start of the experiment was 0.01025 moles/kg, known from mixing the ASW. This was verified by spectrophotometry, and redetermined for each tank after 3 and 4 months. P_{CO_2} was assumed to equal the atmospheric level of $10^{-3.5}$ atm in setting target pH levels for tanks. The ability of the bubblers to achieve this was verified by bubbling laboratory air through deionized water: the pH of the equilibrated water was 6.03 ± 0.02, compatible with the 5.7 ± 0.2 expected for atmospheric pressure (Garrels and Christ 1965). This was later checked by alkalinity determinations.

The pH measurements were made using a Beckman Chem-mate™ digital meter and Beckman combination-type electrode BK39848 precise to 0.01 pH units. The electrode was calibrated on the NBS scale at pH 7.00 before each reading, and calibrated to pH 4.00 and pH 10.00 at least once a week (NBS buffers have a precision of ± 0.005 units). An identical but separate electrode and set of buffer solutions were used for the sterile tanks so as to avoid cross-contamination by Hg.

Bivalve Shells. Two species of marine bivalve molluscs were selected based on microstructural differences in the aragonites naturally exposed on the interior surface of the shell after death. The areas inside and outside the pallial line are, in each species, composed of different but related microstructures and separated by the distinctive microstructure of the pallial line itself (which is the arcuate mantle attachment scar parallel to and just inside the shell margin; table 1). In the northern European nut shell *Nucula sulcata* Bronn, inner and middle shell layers are composed of sheet and stacked nacres, respectively; these are relatively organic-rich microstructures with large (5–10 μm) crystallites of relatively low potential surface area for reaction. In the European cockle *Cerastoderma edule* (Linné), inner and outer shell layers are composed of porcellaneous, complex cross-lamellar and cross-lamellar aragonites, a relatively organic-poor microstructure with fine (0.5–2 μm), relatively high-surface-area crystallites. Organic content was determined experimentally for whole shells (defleshed) by weight loss during ignition (method of Paine [1964] and Price et al. [1976]; 3 hrs in a 500°C muffle furnace) and compared with published values (table 1). Taylor et al. (1969, 1973) reported that the two groups of microstructures differ not only in total organic content, but also in the thickness of the organics that surround crystallites within laminae and that separate successive laminae within shell layers (table 1).

Table 1. Microstructural Characteristics of Experimental Shells

Interior Surface		Exterior Surface	Whole-Shell Organic Content (wt %)	Distribution of Organic Matrix
inside pallial line	outside pallial line			
Nucula sulcata Inner shell layer, of sheet-type nacre; 5–10 μm tablets of aragonite	Middle shell layer of columnar (stacked) nacre; 5–10 μm tablets of aragonite	Outer shell layer of composite prismatic aragonite	3.29 ± .1	relatively thick (.02–1.0 μm) intralamellar and interlamellar organic sheets
Cerastoderma edule Inner shell layer of complex cross-lamellar aragonite; 0.5–2 μm laths of aragonite	Outer shell layer of cross-lamellar aragonite; 0.2–2 μm laths of aragonite	Outer shell layer of cross-lamellar aragonite; 0.5–2 μm laths of aragonite	2.22 ± .1	thin membranes between laths

Notes. Wt % organic content determined by weight-loss during ignition. Crystallite shape and size, and distribution of organic matrix determined by SEM of experimental shells. All values consistent with published data of Taylor et al. (1969, 1973) for same species.

In both species, the adductor muscle scars and pallial line are composed of organic-rich prismatic aragonite (Taylor et al. 1969), but these occupy only small areas of the shell interior. The exterior surfaces of shells were not examined because their condition typically varies widely among individuals in live populations, making it difficult to identify post-mortem deterioration unambiguously.

Small specimens of *Nucula* (avg. 18 mm) and of *Cerastoderma* (avg. 23 mm) were collected from native habitats by the University Marine Laboratory, Millport, Scotland and air-shipped to Chicago. Live populations were held in cold (10°C) seawater aquaria until experimental tanks were ready. Vigorous animals were then carefully disarticulated and adhering tissues carefully removed by hand. Each shell (right or left valve) was numbered uniquely on its outer surface, weighed in ASW, and placed concave-up on the floor of a tank. The interior surface was not allowed to dry out at any time in this procedure, which took only a few minutes per specimen.

Three specimens of each species were sampled from each tank after the following intervals of time: 1, 2, 4, and 7 days, and 0.5, 1, 2, 3, 4, 6, and 11 months. Shells were defleshed and added to tanks in two batches: shells to be sampled after $\geq$ 0.5 months were placed in tanks on day 1, and shells to be sampled after 1 to 7 days of treatment were added on day 21 (total $N = 413$). Weight of shell carbonate (in air, calculated from submerged weights) in each 3-liter reservoir was, at the start of the experiment: 28.36 g in the microbial undersaturated tank (MU; $n = 30$), 25.33 g in the sterile undersaturated tank (SU; $n = 30$), 52.17 g in the microbial saturated tank (MS; $n = 48$), 54.33 g in the sterile saturated tank (SS; $n = 47$), 45.98 g in the microbial supersaturated tank (MSS; $n = 49$), and 41.02 g in the sterile supersaturated tank (SSS; $n = 48$). Shell carbonate added for the short-term experiment during the third week was: MU = 24.55 g, SU = 20.19 g, MS = 28.72 g, SS = 20.89 g, MSS = 35.66 g, and SSS = 19.49 g ($n = 15$ *Cerastoderma* and 12 *Nucula* shells each tank). Because shells were removed permanently when sampled and not replaced, solid to solution ratios decreased steeply from maximum values of ~10g/liter over the course of the experiment.

Sampled shells were immediately weighed in ASW to determine weight loss, rinsed briefly in deionized water, and placed concave-down on laboratory tissue to air-dry for 12 hrs before being coated for Scanning Electron Microscopy (SEM). Interior surfaces of the whole shells were SEM-scanned along a transect perpendicular to the ventral margin, avoiding adductor muscle scars. An additional set of untreated shells was examined by SEM to establish the initial, "pristine" state of shell microstructures. Because of possible anaerobiosis and shell corrosion during the stress of air-shipment and holding tanks, this post-shipment condition is the most appropriate baseline for evaluating subsequent experimental deterioration.

Another set of fresh shells was used to establish the SEM signature of various reagents known to attack different parts of shell structure (Mutvei 1984; C.A. Richardson 1991 pers. comm. for Protease). To simulate the selective removal of organic matrix, shells were immersed for periods of either 1.5–2.5 hrs in a 8–12% solution of sodium hypochlorite or for 3–5 days in a 1mg/ml solution of the enzyme Protease K. To simulate selective attack on mineral crystallites, fresh shells were immersed for periods of 1–3 days in 25% solutions of gluteraldehyde, which both decalcifies carbonate minerals and fixes proteins. To examine the effects of aging in atmosphere, simulating museum storage, an additional set of shells was left to dry uncovered on a laboratory bench for 11 months.

Changes in Water Chemistry during the Experiment

Trends in pH. All tanks fluctuated daily in pH (figure 1). Fluctuations were generally on the order of only a few hundredths of pH in the saturated and supersaturated tanks, that is, within the resolving power of the electrode. Fluctuations were larger and more frequent in the undersaturated tanks (~0.15 pH units, generally between pH 7.75 and pH 7.90): within a few hours after establishing undersaturated conditions by acid-titration, pH would rise as the ASW began to re-equilibrate toward supersaturation. The designation "undersaturated" thus indicates only that the ASW was at target pH for undersaturation ($\Omega_{arag} = \sim 0.5$) for a few hours each day, followed by a rise to near-saturation ($\Omega_{arag} = \sim 0.8$) over the next 24 hrs. In each of the tanks, the largest excursions in pH were related to known perturbations, such as the temporary failure of a bubbler, the addition of shells for short-term experiments at the beginning of week 3, or the addition of fresh ASW or of deionized water to correct reservoir volume and salinity.

Trends in Ca^{++}. Analysis of major ions after 3 months revealed an increase in concentrations, presumably due to evaporative loss of water. Thus, although pHs were relatively steady, saturation levels would have risen over this period in response to the increase in Ca^{++} (figure 1). The time

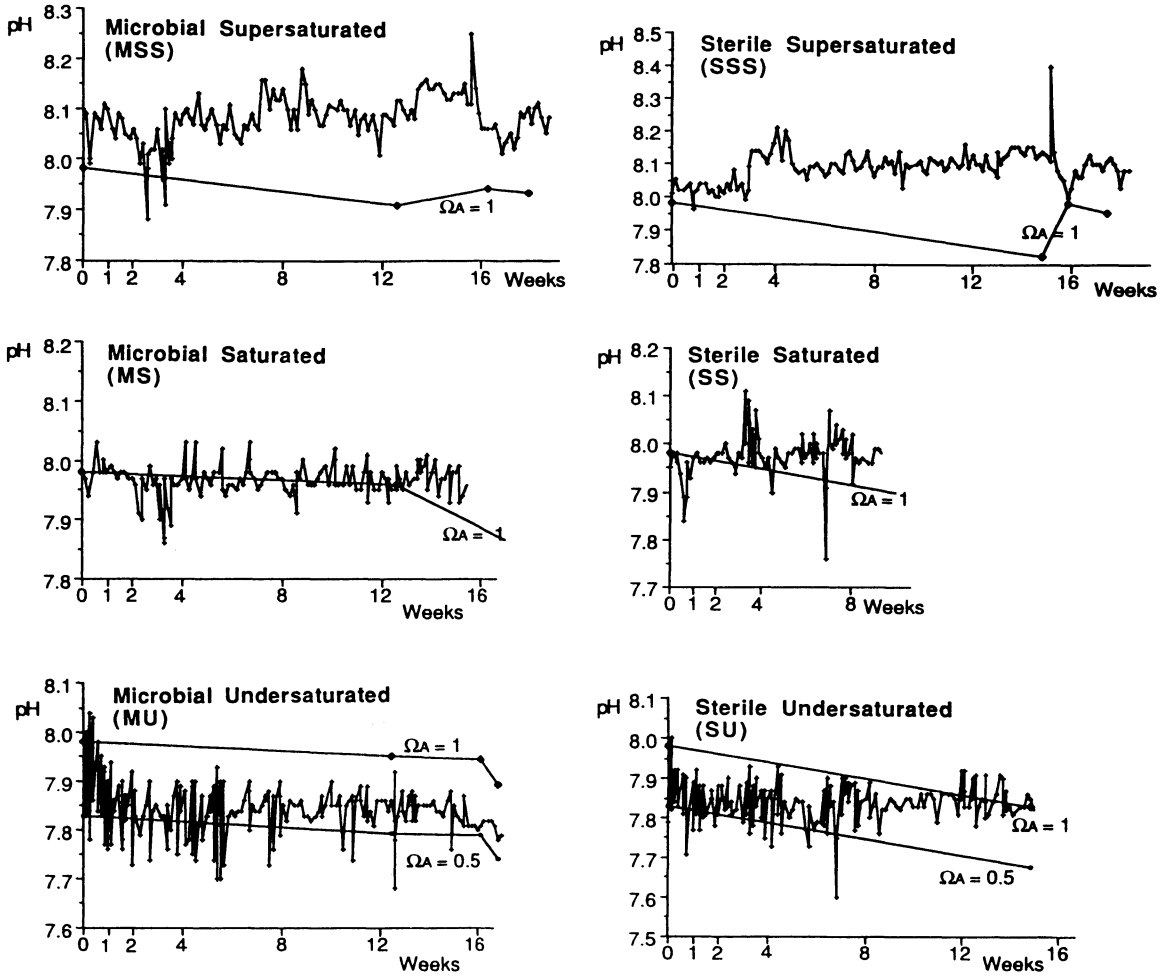

Figure 1. Daily pH readings (both before and after acid-titrations) during the first 4 months of the six experimental tanks. Although target pH levels are maintained within ± 0.1 pH units, waters are calculated to have drifted to higher than target saturation states (Ω_{arag} = 0.5, ~1, and >1 for undersaturated, saturated and supersaturated tanks) because of evaporative increase in $[Ca^{++}]$. Ω_{arag} contours assume that $[Ca^{++}]$ increased linearly and that water remained equilibrated with atmospheric CO_2.

course of evaporation is not known, and thus is plotted on figure 1 as a straight line. As a correction, tanks at 3 months were diluted to their original levels by factors of 1.30 to 1.52 in microbial tanks, and by 1.74 and 3.45 for sterile tanks. Evaporation was a greater problem in sterile tanks because these were kept under an exhaust hood. Dilutions required at subsequent one month intervals were much smaller.

Trends in Alkalinity. There is also evidence that the P_{CO_2} and total alkalinity of the ASW also increased over time, based on the slowing rate of acid-titration necessary to maintain target pHs in the undersaturated and saturated tanks (figure 2). An alkalinity determination at 5 months indicated that the undersaturated tanks were actually at Ω_{arag} = 0.9 by this time, even when pH was at the target level of 7.83. Alkalinity buildup probably indicates inefficient scrubbing of CO_2 by bubblers. The time course of increasing alkalinity is not known.

Water Saturation. Supersaturated conditions appear to have prevailed in microbial and sterile supersaturated tanks over the full 11 month period. ASW maintained a high pH without intervention, with a calculated Ω_{arag} of 1.1 for the first week and >2 thereafter (figure 1). There was a slight drop in saturation from freshly mixed ASW during the first week. This may reflect precipitation of $CaCO_3$ on newly introduced shells, which is common in reaction vessels (L.M. Walter pers. comm.), or may have been caused by decay of organic coatings on shells.

Undersaturated tanks received more acid than other tanks during the first 2 months of the experi-

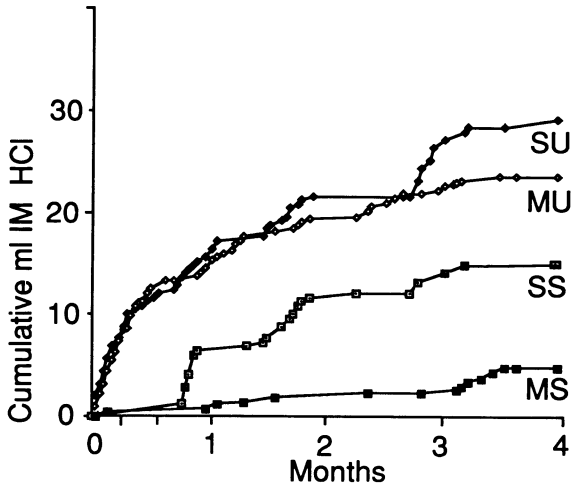

Figure 2. Undersaturated tanks (SU and MU, sterile and microbial respectively) required higher cumulative acid-titrations to maintain target pHs than did saturated tanks (SS and MS), but acid demand generally reached a plateau after the first 2 months. Supersaturated tanks required no pH adjustments.

ment (steepest parts of MU and SU curves in figure 2), and thus ASW in these tanks should have been relatively undersaturated during this period. However, the most conservative interpretation of the acid-addition curve (figure 2) is to assume that conditions of virtual saturation existed in the undersaturated tanks at least as early as ~day 60, when the curve reached a plateau, owing to increasing alkalinity. Assuming a liberal error of ±10% for P_{CO_2}, the calculated error in Ω_{arag} would have been ±17%, meaning that undersaturated tanks may have had minimum saturation levels of ~0.6 rather than 0.5, and risen each day to ~0.9 rather than 0.8. These fluctuations are comparable to those produced by natural diurnal and seasonal processes.

Because of analogous trends in the rate of acid-addition and in Ca^{++} and alkalinity levels, we suspect that ASW in the microbial and sterile saturated tanks was probably saturated for only the first 1–2 months, thereafter rising to fully supersaturated conditions (figures 1 and 2). After this initial period, the chemistry of saturated tanks cannot be distinguished from their companion supersaturated tanks. Consequently, only the first 2 months of SEM and weight-loss data from the undersaturated and saturated tanks are considered valid. Data collected after 2 months in the saturated tanks are combined with their supersaturated counterparts.

Experimental Deterioration of Organic-Rich Nacreous Aragonites

Initial Condition. Interior surfaces of freshly dissected *Nucula* shells had a distinct 200 μm wide pallial scar. The inner shell layer (inside the pallial band) was characterized by smooth, broadly overlapping shell laminae composed of a single layer of completely sutured 5–10 μm diameter tablets (sheet nacre). Isolated tablets occurred along the horizontally growing edges of laminae and were subcircular, diamond-shaped, or hexagonal in outline (figure 3*a*). In small areas on a few specimens, isolated tablets were irregular or elongate in outline and even perforate in small areas. This damage probably reflects metabolic stress associated with collection, shipping, or holding of live animals.

The middle shell layer (outside the pallial band) was characterized by tablets stacked 2–4 high into columns and elongated mesas. This stacked nacre had maximum relief toward the shell margin and rested on a smooth sublayer of completely fused aragonitic tablets. Near the pallial band, where tablets had not all joined into continuous laminae, tablets were smooth-edged and subcircular, diamond-shaped, or hexagonal in outline.

Damage Inside the Pallial Band. Sheet nacre deteriorated through a series of stages when examined at 2000× (figure 3*b,c,d*). The same sequence was observed in all tanks, but the rate at which it progressed and thus the cumulative damage to shells during the experimental period varied according to saturation state and microbial activity (figure 4).

Damage stages are assigned descriptive names and scaled arbitrarily from 0 to 4 in figure 4. The six tanks are designated: MU = microbial undersaturated; SU = sterile undersaturated; MS = microbial saturated; SS = sterile saturated; MSS = microbial supersaturated; and SSS = sterile supersaturated.

Pristine (0): No detectable change from condition at start of experiment.

Reticulated Sheets (1): The first microstructural damage was the development of a reticulated (net-like) pattern on the surface of shell laminae. These lines were either dark shadows or brightly charged under SEM and corresponded to organic-rich sutures between aragonitic tablets, which remained pristine in outline and surface condition. Reticulated fabric was first seen in MU specimens after just a few days (figure 3*b*), and dominated the area inside the pallial line by 2 weeks. It was not observed until the one-month sampling in MS, MSS, and SU specimens, and not until 4 months in SS and SSS specimens (figure 4).

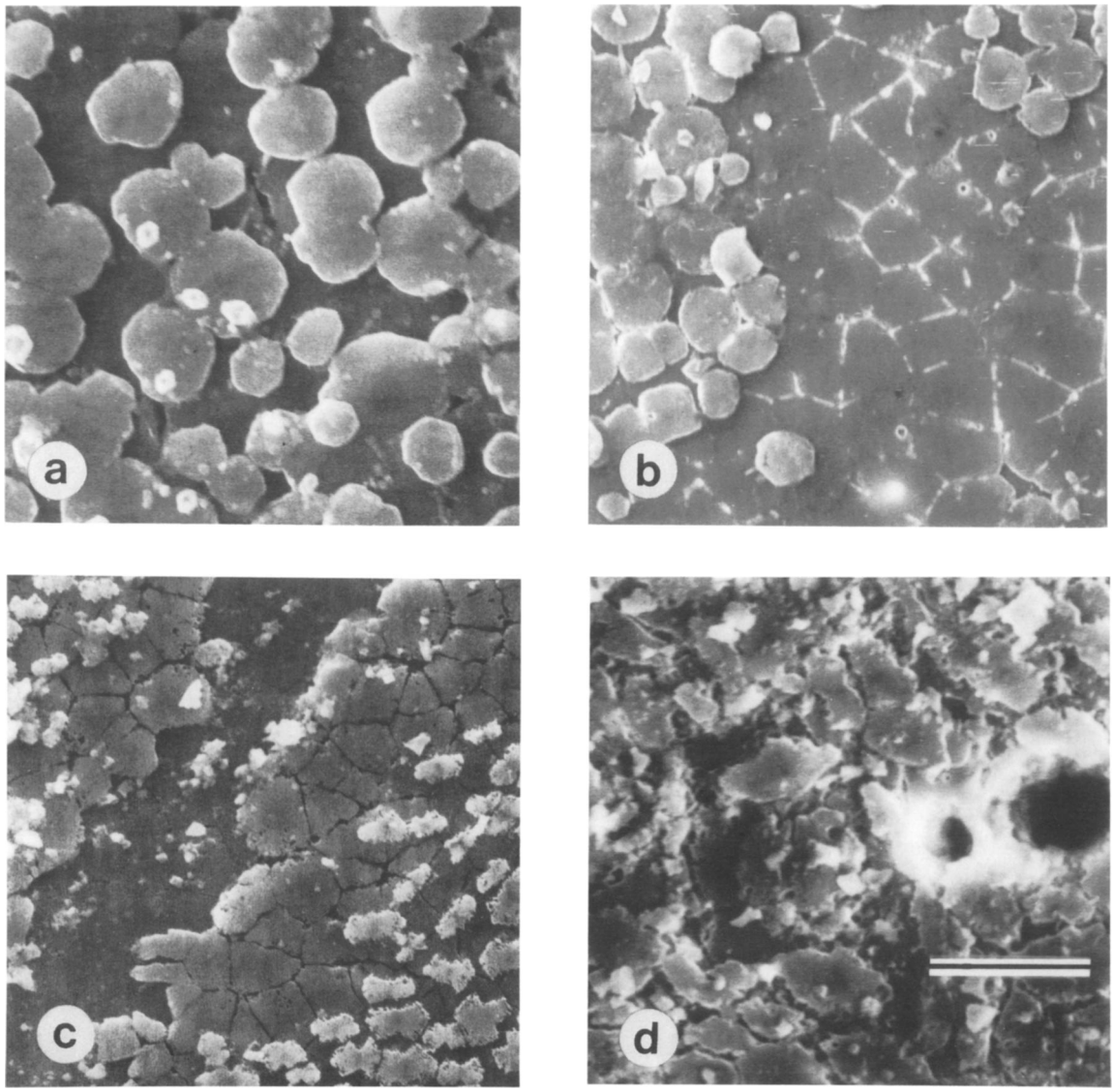

Figure 3. Sequential stages, numbered 0 to 4, in the deterioration of organic-rich sheet nacre inside the pallial line of *Nucula sulcata,* based on 2000× SEM of shells sampled from the microbial undersaturated tank. (*a*) Pristine condition (stage 0), individual tablets are tightly fused within sheets; freshly dissected specimen, no treatment. (*b*) Organic sutures between roughly hexagonal tablets are highlighted in SEM images, producing a reticulated (net-like) surface pattern even though tablets remain tightly fused (stage 1); specimen removed after 1 day. (*c*) Spaces between tablets enlarge, via a series of coalescing pits along suture lines, into steep-walled canyons which leave tablets isolated from one another (stage 2); the edges of tablets become finely scalloped or perforate (≤1 μm scale; stage 3); specimen removed after 1 month. (*d*) Further damage to the sutural edges of tablets produces a jagged surface on the original sheet (stage 4); specimen removed after 2 months. Scale = 10 μm.

Canyoned Sheets (2), ± Cuspate Tablets (3): The reticulated pattern is incised into the surface, usually via a series of ≤0.5 μm-diameter pits that coalesce into an intersecting system of steep-walled canyons. Originally coherent shell laminae are transformed into horizons of discrete tablets. The edges of these tablets eventually become sharply cuspate or perforate at a submicron-scale. Canyons and edge-perforations were well developed by one month in the MU specimens (figure 3*c*). Canyons were clear by two months in MS and MSS specimens, but had only begun to appear by that time in SU specimens and did not appear in SS and SSS specimens even after 11 months (figure 4).

Jagged Tablets (4): An irregular, jagged shell sur-

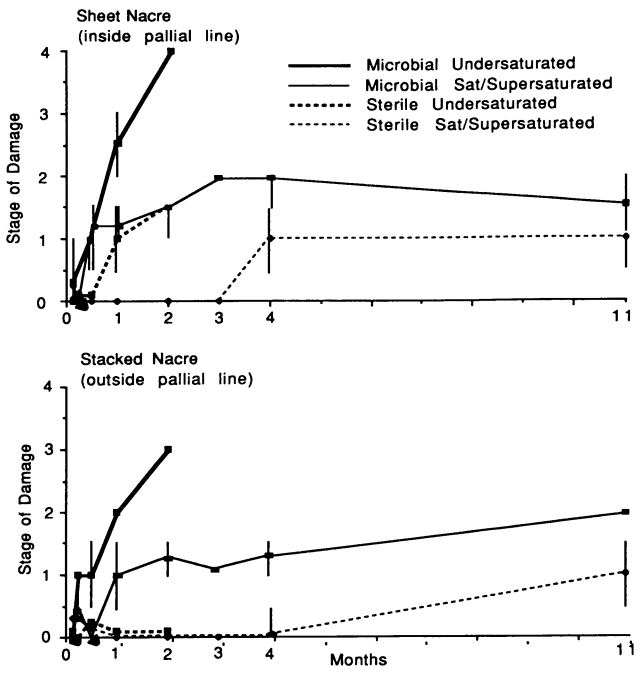

Figure 4. Nacres deteriorated through the same stages in each tank (as illustrated in figure 3), but the rate of deterioration varied. For sheet nacre inside the pallial line, rates varied such that deterioration of MU specimens > [MS, MSS, and SU specimens] > [SS and SSS specimens]. Stacked nacre outside the pallial line deteriorated more slowly, but relative rates among tanks were similar: MU > [MS and MSS] > [SU, SS, and SSS]. Vertical bars through data points indicate range in damage among sampled specimens.

face was produced by more extreme damage to the edges and, to a lesser extent, to the upper surfaces of tablets. Some tablets appeared to be loosened entirely from the microstructure. Jagged tablets were common by 2 months in MU specimens (figure 3*d*), and a few small areas of this damage were observed by 2 months on one SU shell that was otherwise dominated by reticulated sheets and incipient canyons. Jagged tablets never appeared in any of the saturated or supersaturated specimens.

The overall ranking of tanks based on damage inside the pallial line was MU > [MS, MSS and SU] > [SS and SSS] (figure 4).

Damage Outside the Pallial Band. Microstructural deterioration started along the pallial edges of shell laminae and advanced as a front toward the shell margin. This proceeded fastest in MU tanks, where canyons had advanced to the shell edge by 2 months, next fastest in MS and MSS tanks, and slowest in sterile tanks where damage was limited to reticulation along the pallial line even after several months (figure 4). The overall ranking of tanks was MU > [MS and MSS] > [SU, SS and SSS].

Other Damage. At 200×, the most dramatic change to the shell interior was the appearance, within 2 weeks, of ~10 μm-diameter boreholes of presumed microbial origin (figure 5). These appeared only in microbial tanks and in all microbial tanks regardless of saturation state. Holes had circular cross-sections and sharp edges, were hyperdistributed (although a few cross-cutting examples were observed), and showed no particular relationship to crystallites or sutures. Over a 4 month period, they increased in diameter up to 15–20 μm and also became more abundant (up to 3.5 per 100 μm × 100 μm area). Although they typically appear as black holes in SEM images, commonly with highly charged edges, a few down-hole views showed that they penetrate multiple shell laminae and are sinuous. Macroscopically, the only change to interior surfaces was some loss of surface sheen. This correlated with the development of canyoned nacre.

Comparison of Nacres. In general, stacked nacre outside the pallial band deteriorated more slowly than sheet nacre inside the pallial band, commonly lagging by one stage at each sampling interval (figure 4). The ranking of tanks according to rates of deterioration was also slightly different, with sterile tanks lagging behind all three microbial tanks, and boreholes were less densely spaced than for sheet nacre inside the pallial line.

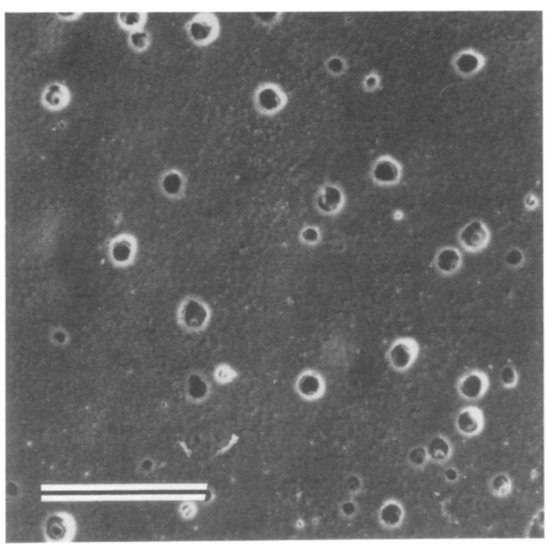

Figure 5. Microbial (probably fungal) borings in sheet nacre of *N. sulcata* after 4 months of treatment in microbial supersaturated seawater. Borings appeared within 2 weeks of treatment in all microbial tanks, and over time became larger and more densely spaced. Scale = 100 μm.

Experimental Deterioration of Organic-Poor Porcellaneous Aragonites

Initial Condition. The pallial line appeared only as a slight change in slope on the interior surfaces of freshly dissected *Cerastoderma* shells. The entire interior surface did not reveal any structure at 2000–3000×. Based on its behavior in experimental tanks, the interior was coated by a thin (one crystallite thick?) layer of irregular 1–2 μm granular crystallites (homogeneous microstructure of Taylor et al. [1969]). Cross-lamellar and complex cross-lamellar microstructures, composed of tightly-packed 0.5 μm laths dipping in opposing or radial directions respectively, were not observed until this surficial layer had been stripped. Interior surfaces showed no evidence of pitting or corrosion from metabolic stress.

Damage Inside the Pallial Line. Microstructural damage did not appear over the entire area at once, but started in scattered spots which then expanded outward (seen at 200×). Damage within patches proceeded through a series of stages (figure 6). The same sequence was observed in all tanks, but the rate and cumulative damage varied among tanks (figure 7). Damage was described in terms of the intensity of damage within patches (seen at 2000×) and the approximate area so affected (seen at 200×). Damage stages were assigned descriptive names and scaled arbitrarily from 0 to 4.

Pristine (0): No detectable change from condition at start of experiment.

Creviced Surface Coat (1): The first microstructural damage appeared as patches of fine-scale (submicron) roughening (200×). At 2000×, these patches were characterized by irregular crevices along the organic-rich sutures of 1–2 μm irregular crystallites, and by scattered holes comparable in size and shape to crystallites or small groups of crystallites (figure 6*a*). The shell layer that exhibited this style of damage appeared to be a single lamina only one crystallite thick. This damage appeared within a few days in all treatments except the SS and SSS tanks, where it was rare for the first 2 to 4 months (figure 7).

Laths Exposed (2): Removal of the surficial shell coat revealed 0.5–1.0 μm-long, lath-shaped crystallites dipping at a low angle to the shell surface (cross-lamellar microstructure). Laths were oriented approximately parallel to each other, and stood out in positive relief because of steep-sided canyons along suture lines (figure 6*b*). This stage was observed by 4 days in some patches on MU specimens, by 2 weeks in MS, MSS, and SU specimens, and was never seen in SS and SSS specimens (figure 7).

Radial Laminae Exposed (3): At 200×, the surface appeared pristinely smooth but a low-relief (a few microns) mounded topography had developed, with crests spaced ~20 μm apart. At 2000×, these hills consisted of radially dipping shell laminae that were each a few tenths of a micron thick and that imparted a surface pattern of arcuate swirls (complex cross-lamellar microstructure; figure 6*c*). Crystallites within laminae were tightly packed and fused, without sutural crevices or canyons. This stage dominated MU specimens by 1 week, dominated SU, MS and MSS specimens by 1 month, and was never observed in SS and SSS specimens (figure 7).

Coarse Blocks (4): Where deterioration had advanced most deeply below the shell surface, a relatively coarse microstructure of 2–3 μm roughly rhombic blocks was exposed (figure 6*d*). This may be a form of complex cross-lamellar structure (cf. Taylor et al. 1969). A few blocky patches appeared within 2 weeks in MU specimens and dominated the surface of some specimens by 1 month, whereas this stage did not dominate MS and MSS specimens until 2–3 months and was never significant in SU, SS, and SSS specimens (figure 7).

The overall ranking of tanks for damage inside the pallial line was MU > [MS, MSS and SU] > [SS and SSS] (figure 7).

Damage Outside the Pallial Line. Microstructural damage was more difficult to detect outside the pallial line, and the stage with parallel laths (2) was not observed. Despite uncertainties (indicated by missing data in figure 7), deterioration proceeded fastest in MU, MS, and MSS tanks, much slower in the SU tank, and slowest in SS and SSS tanks where some shells remained pristine for 3 months. The pallial line itself and the edges of internal ribs were roughened, exposing coarse blocky microstructure.

Other Damage. *Cerastoderma* shells in microbial tanks were bored in the same way as were *Nucula* shells (figure 5). However, boreholes were initially smaller (<5 μm), attained smaller maximum sizes (≤ 10 μm), were slower to appear (2 months), and remained sparse (maximum 0.8 per 100 μm × 100 μm area).

Comparison of Porcellaneous Microstructures. In general, cross-lamellar aragonite outside the pallial line deteriorated more slowly than complex cross-lamellar aragonite inside the pallial line, lagging by as much as one stage at each sampling interval (figure 7). The ranking of tanks was slightly different, with sterile tanks lagging behind all three microbial tanks, and boreholes were less densely spaced than inside the pallial line.

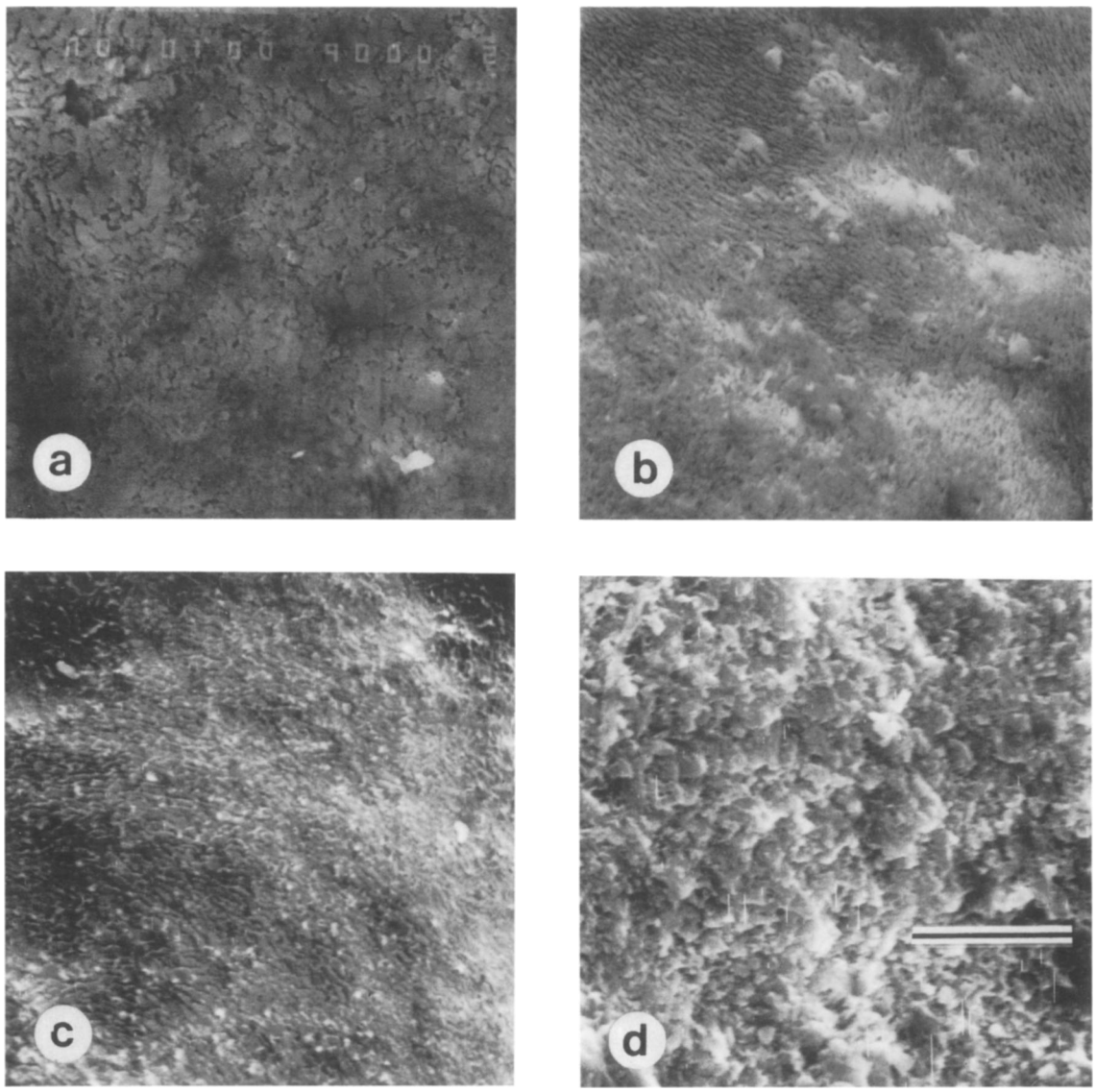

Figure 6. Sequential stages, numbered 0 to 4, in the deterioration of organic-poor porcellaneous aragonites from *Cerastoderma edule*. Deterioration began in small patches, expanding outward and down into successively deeper sublayers over time. Pristine specimens (stage 0) exhibited a smooth, featureless surface when examined at 2000× SEM. (*a*) Crevices developed along sutures between 1–2 μm irregular crystallites in a surficial, single-crystallite layer of homogeneous microstructure (stage 1). (*b*) Steep-walled canyons developed along suture lines in the underlying cross-lamellar microstructure, exposing individual 0.5 μm mineral laths on the shell surface (stage 2). (*c*) Exposure of radially arranged sheets of complex cross-lamellar structure, with laths still tightly fused (stage 3). (*d*) Exposure of relatively coarse, rhombic crystallites (a form of complex cross-lamellar aragonite?) (stage 4). Scale = 10 μm.

Simulation of Experimental Damage

Organic-Rich Nacreous Aragonites. Bleach and protease, which selectively remove organic matrix from shell, had little effect on the pallial band of *Nucula*, but otherwise replicated in form and scale the reticulated, canyoned, and cuspate damage observed in experimental shells (figure 8*c*, *d*). Damage was greatest inside the pallial band, as also observed in experimental shells. Exposure to laboratory air for 11 months (dehydration and oxidation) also produced reticulated and canyoned damage similar to experimental shells (figure 8*e*).

Decalcification by gluteraldehyde uniformly corroded nacre, leaving a granular texture. Even the mildest treatment produced pits across the entire upper surfaces of sheets (figure 8*a*), unlike experimental shells where damage was focussed exclusively on tablet edges, with upper surfaces of tablets remaining smooth. Longer treatment pro-

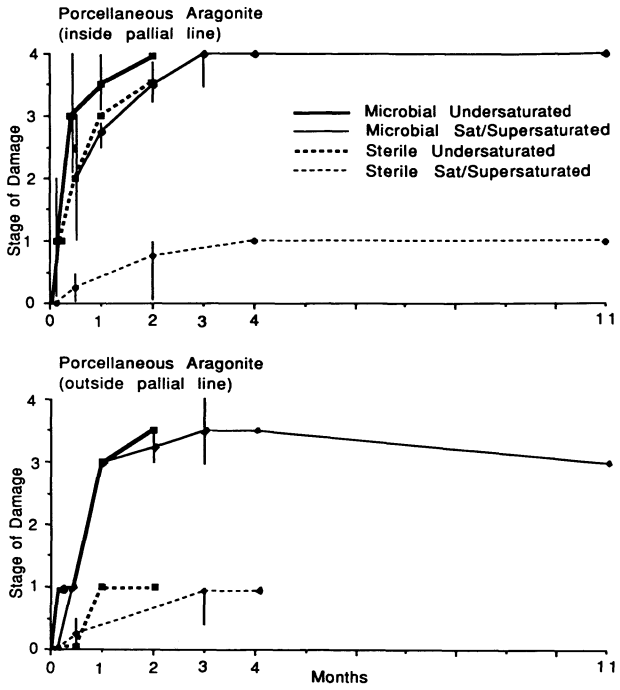

Figure 7. Organic-poor porcellaneous aragonites deteriorated through the same stages in each tank (as illustrated in figure 6), but the rate of deterioration varied. Inside the pallial lines, rates were MU ≥ [MS, MSS, and SU] > [SS and SSS]. Shell outside the pallial line deteriorated more slowly, but relative rates among tanks were similar: [MU, MS, and MSS] > [SU, SS, and SSS]. Vertical bars through datapoints indicate range in damage among sampled specimens.

duced an irregular surface in which the original shape of the tablets was largely obliterated (figure 8*b*). This was an extreme form of the jagged tablets observed in experimental shells (e.g., figure 3*d*). Gluteraldehyde damage was most severe outside the pallial line, opposite to the pattern in experimental shells.

Organic-Poor Porcellaneous Aragonites. Protease damage to *Cerastoderma* was virtually indistinguishable in type and distribution to experimental damage. Damage was patchy at 200×. The smoothest areas revealed, at 2000×, either parallel laths separated by sutural crevices (stage 2) in experimental shells, as in figure 6*b*) or radial laminae (stage 3, as in figure 6*c*). The roughest patches were exposures of an underlying coarse-grained microstructure (stage 4, as in figure 6*d*). Crystallites stood in positive relief across the entire surface, with undamaged edges. Protease caused more damage inside than outside the pallial line and roughened the pallial line dramatically as in experimental shells.

Gluteraldehyde uniformly roughened the entire surface inside the pallial line (at 200×) and also produced some deep (10 μm), irregular pits. Such pitting was pervasive outside the pallial line, contrary to experimental shells where damage (including microbial boreholes) was greatest inside the pallial line. Gluteraldehyde had little effect on the pallial line itself, in contrast to experimental shells.

Experimental Weight Loss

Shells in undersaturated tanks were more likely to show weight loss than shells in saturated and supersaturated tanks, which were unchanged or gained in weight (Mann-Whitney U-test, $0.05 < p < 0.10$ for *Nucula* and $p < 0.025$ for *Cerastoderma;* based on the most reliable samples: pooled MU and SU data at 1 month versus pooled MS, MSS, SS, and SSS data at 2 months). In general, however, cumulative weight changes were small (≤1% even at 4 months), variance was high, and numbers per sampling were necessarily small despite the large total number of shells in the experiment. Consequently, no other differences, such as between microbial and sterile tanks at a given Ω_{arag} or between organic-rich and organic-poor shells within a tank, proved significant.

Discussion

Shared Pattern of Organic Influence. The SEM time-series data showed the same pattern of deterioration in all tanks, and comparison with simulated damage showed that deterioration was limited initially to decomposition of organic matrix. The retreat of matrix left crystallites in positive relief and permitted these to detach from the shell surface, both singly and in small groups. For all microstructures in all tanks, this loss of organic matrix was the rate-limiting step in shell deterioration. Only the rate of deterioration varied among tanks.

Dissolution must have occurred in undersaturated tanks, since water pH rose in response to acid-addition, but in situ crystallites generally remained pristine. Waters thus did not attack microstructure directly, and dissolution must have been focussed instead on particulate matter released from the shell surface. The only exception to this was scalloping and perforation of nacre tablets in the microbial undersaturated tank. This damage is a form of dissolution, but the fact that it was encountered only in microbial tanks and was limited to sutural edges suggests that dissolution was linked to the process of matrix decomposition, probably via high CO_2 produced by microbial respiration of adjacent matrix. Pervasive pitting and

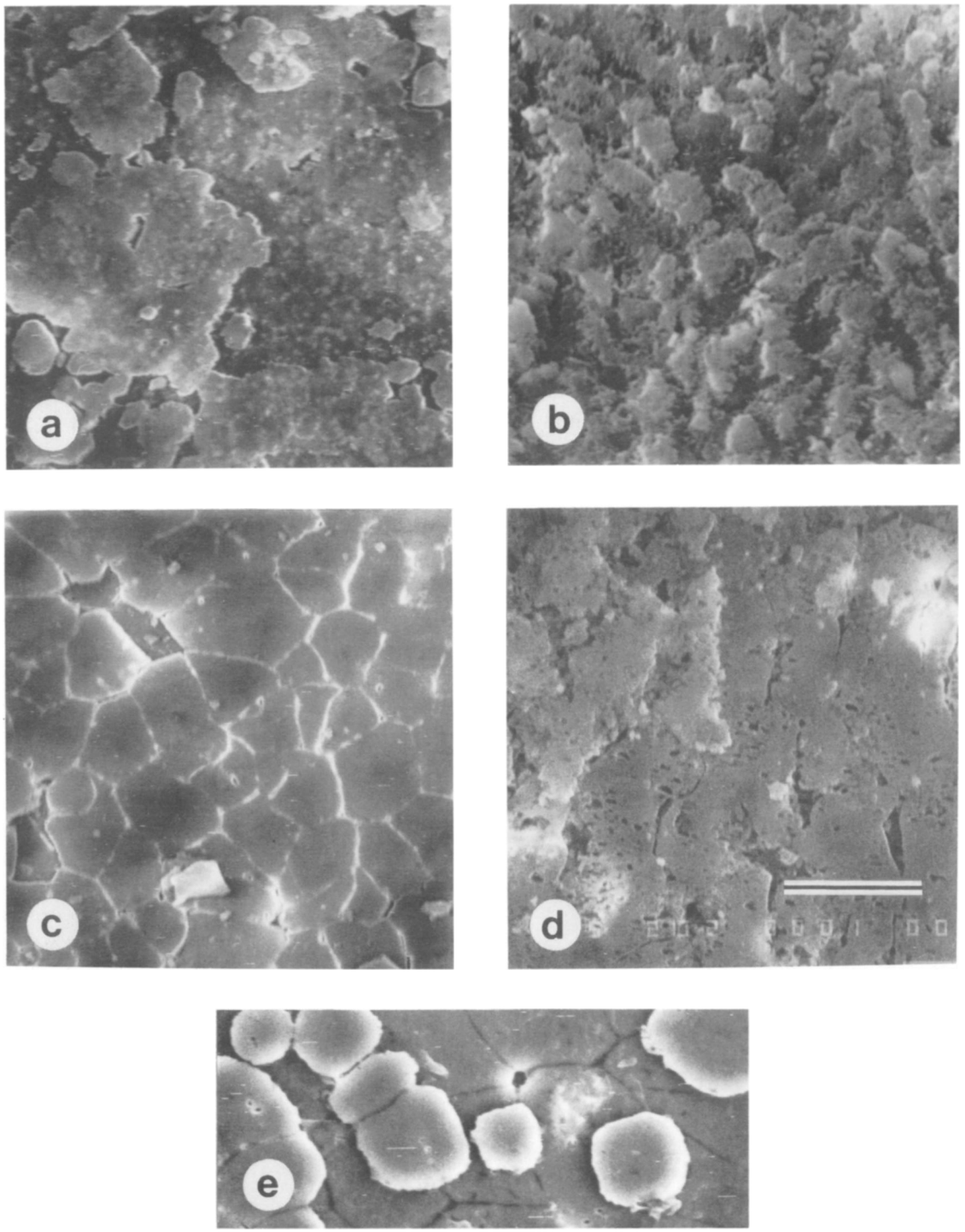

Figure 8. Damage to sheet nacre by reagents of known effect. Decalcification (simulated corrosion) by gluteraldehyde produces fine-scale granulation of upper surfaces of sheets (*a*) and alters outlines of tablets into jagged, irregular shapes (*b*), although to a more extreme stage than observed in experiments (compare with figure 3*d*). Selective removal of organic matrix by sodium hypochlorite or by protease produces reticulated surfaces (*c*) and finely cuspate canyons and perforations (*d*) that are closely comparable to experimental damage (figures 3*b*,*c*). (*e*) Exposure to atmosphere (11 months) selectively damages organic matrix, isolating tablets within originally continuous sheets. Scale = 10 μm.

granulation typical of chemical (gluteraldehyde) attack was not observed during the course of the experiment, but relatively prolonged exposure (≥2 months) in the microbial undersaturated tank did produce some corrosion of nacre tablets in superficial shell laminae. This may reflect direct interaction between seawater and in situ crystallites, but it was limited to laminae in a relatively late stage of matrix loss.

The fact that rates of deterioration were ≥2× higher in microbial than in sterile tanks at any given saturation state, and were as high or higher in microbial saturated and supersaturated tanks than in sterile *under*saturated tanks, underscores the controlling influence of organic matrix on the reactivity of fresh shells. Organic coatings and matrix must be decomposed before crystallites become vulnerable to dissolution by ambient waters, and thus the initial role of organics is protective. Upon decomposition of organics, whether by hydrolysis or by microbes, microstructures disintegrate by detachment of crystallites. In microbial waters, destruction is presumably furthered by respiration along crystalline sutures and by borers, which both undermine microstructure and increase its reactive surface area. During shell aging, therefore, organics apparently shift to making microstructures more vulnerable to physical disintegration and to bioerosion, and fuel dissolution by serving as a microbial substratum. Microbial respiration alone could not cause dissolution of an entire shell, given that even organic-rich microstructures contain only a few percent organics, but it might have a disproportionate effect given its proximity to crystallites.

This pattern is comparable to that reported for biogenic carbonates in natural environments. Alexandersson (1975) reported that "organic templates of skeletal carbonates disappear together with, or even slightly before, the mineral substance" in mollusk shells from the Skaggerak, thus weakening structurally complex grains and permitting physical deterioration of microstructures. He attributed organic loss to "leaching," and etching of in situ crystallites to undersaturation of Baltic waters. Lewy (1975, 1981) attributed these same features to microbial attack and its attendant high-CO_2 conditions (and see Gaspard 1989 and Simon and Poulicek 1990). Heinrich and Wefer (1986) found that decomposition of diatom-rich surface coatings and cell walls and mechanical disintegration were more important than chemical dissolution in some taxa in undersaturated waters, based on specimens suspended for 52 days in the Drake Passage: that is, shells did not dissolve until they had been cleaned of organics. Roux et al. (1989) similarly found significant biocorrosion and evidence of organic-loss (loosened crystallites) in aragonitic pelecypods after 3 yrs of exposure below the aragonite CCD, but no trace of aragonite dissolution.

Our experiments demonstrate that hydrolysis and leaching (Hudson 1967; Alexandersson 1975) are only of secondary importance to microbial decomposition in destroying organic matrix. Microbial deterioration proceeds 2 to 10× faster than abiotic processes in sterile aerated waters of comparable saturation, and only our microbial rates match the rapid rates of matrix loss documented in natural waters (e.g., Heinrich and Wefer 1986; Jensen and Thomsen 1987; Simon et al. 1990).

Effect of Water Saturation. Hypothetically, organic matrix should be vulnerable to microbial decomposition regardless of water saturation state, as suggested by Lewy (1981). Our experiments support this: shells deteriorated via organic loss in all tanks. Saturated and supersaturated waters thus should not be regarded categorically as taphonomically neutral, given the potential for organic loss and consequent physical dissociation of crystallites. We have found examples of total organic loss in shells dredged from modern death assemblages (figure 9). These wet, organic-free shells had the flexible consistency of cardboard (and see Emig 1990 for brachiopods).

However, although saturation state does not determine the pathway of deterioration for fresh shells, our experiments indicate that it does influence the rate: microstructural deterioration rates were ≥2× faster in microbial undersaturated tanks than in other microbial treatments (deterioration was also higher in sterile undersaturated than in other sterile treatments). Undersaturated waters presumably are more effective in ridding shell surfaces of loosened or partially exposed crystallites, thereby more fully exposing matrix in underlying shell laminae to microbial attack (or hydrolysis). Undersaturated waters should also create less of a concentration gradient drawing matrix-sourced CO_2 away from the shell surface.

Alexandersson (1978) reported that organic-loss did not seem to be particularly important in tropical supersaturated waters, and many authors have noted that carbonate grains have shiny rather than dull surfaces in such settings. In these shallow-water environments the effects of organic-loss are perhaps masked by more aggressive algal microboring (1–10 μm scale) with attendant micritization, or perhaps the sub-micron voids created by matrix loss are quickly filled by mineral precipitates. The

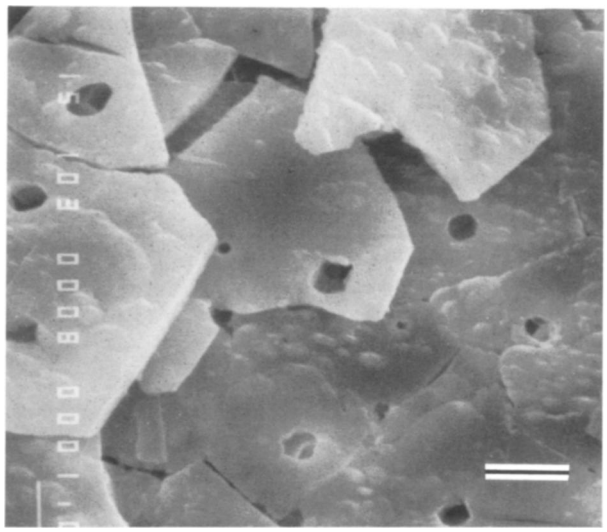

Figure 9. SEM of Recent nuculoid bivalve *Acila castrensis* (Hinds) dredged dead from pebbly mud in Puget Sound, Washington. Nacreous sheets have lost their organic matrix, but tablets are otherwise in excellent condition and remain in approximate microstructural order. Macroscopically, these shells had slightly dulled surfaces, were somewhat flexible under pressure, and in some instances could be dissociated into crystallites by running them between the fingers. Boreholes are at the small end of the variance observed in experimental shells (figure 5) and are probably fungal in origin. Scale = 1 μm.

role of organic matrix in carbonate grain destruction in these settings deserves re-examination.

Differences in Vulnerability of Microstructures. Given experimental evidence for the changing role of organic matrix during shell aging, the net effect on shell preservation during time-averaging is not deductively obvious. On the one hand, one might expect that organic-rich shells have relatively high preservation potential since matrix limits direct interactions between crystallites and water (Kennedy and Hall 1967). On the other hand, organic-rich shells might have lower preservation potentials (Emig 1990; Simon et al. 1990): the more dependent the microstructure upon organic-binding of crystallites, the more vulnerable it should be to physical disintegration as organics are lost, and organic-rich microstructures might preferentially attract microbial decomposers and microborers.

In our experiments, deterioration in a given tank was visually more striking in organic-rich nacres (*Nucula*) than in organic-poor porcellaneous aragonites (*Cerastoderma*), but this is difficult to quantify. However, 1–10 μm-scale microbial boring was quantifiable: organic-rich microstructures were colonized ~4× faster and ~4× more intensely than organic-poor types. Gaspard (1989), Roux et al. (1989), and Simon and Poulicek (1990) also found positive relationships between rate of biocorrosion and organic content, lending further support for Poulicek's (1983) suggestion that microbes exploit intraskeletal organic matrix as an energy source. Such preferential colonization would be a contributing factor in lowering the preservation potential of organic-rich taxa.

Slight differences in the reactivity of microstructures found inside and outside the pallial line in each taxa (figures 4 and 7) may also reflect differences in matrix—e.g., its total weight %, the proportion of soluble and insoluble molecules, or the physical interconnectedness of sheaths—but this needs to be tested. It might also reflect the different functions of mantle tissues in these areas and thus the condition of the shell surface at the time of death. Inside the pallial line where the mantle is closely associated with acid-base metabolism, shell material is periodically corroded to buffer body fluids (Lutz and Rhoads 1977; Crenshaw 1980). This *pre*-mortem history (and the absence of a surficial organic coating?) might cause the inner shell layer to be more reactive to post-mortem attack than the surface outside the pallial line, where shell deposition is highest during life (Crenshaw 1980).

Between-taxon differences in weight loss (≤0.36% change per sampling) were statistically insignificant (Mann-Whitney U test, $0.10 > p > 0.05$ for pooled undersaturated data). However, it is probably meaningful that the relatively organic-poor *Cerastoderma* shells at most only matched the weight loss of organic-rich *Nucula*, given the finer crystallites (0.5 μm vs. 5–10 μn in nacre) and thus the greater potential surface area for mineral reaction. The fact that low-surface area *Nucula* shells had weight-losses comparable to those of high-area *Cerastoderma* is consistent with SEM evidence that organic matrix is more important than the mineral phase in determining reaction rates in fresh shells, and that the overall effect of organic matrix in microbially active environments is to increase a shell's vulnerability to post-mortem destruction.

This conclusion can be tested independently by comparing the composition of death assemblages with source communities. For example, in Valentine's (1989) data for living and Pleistocene marine bivalves of California, only 48% of the 54 living species with predominantly nacreous shells occur in the fossil record, whereas 84% of the 185 living

species with non-nacreous aragonitic shells are preserved as fossils ($p < 0.001$, G-test). Although some nacreous species also have small bodies and low population densities that would contribute to lower preservation potentials, as discussed by Valentine, nacreous species are not exclusively small and sparse and these characteristics are also common to many non-nacreous aragonitic taxa.

Implications and Conclusions

Dynamics of Early Diagenesis. The observation that dissolution does not proceed until organics retreat from mineral crystallites suggests that the dynamics of dissolution for fresh biogenic carbonates may differ significantly from the behavior of organic-free sedimentary grains, which show high initial dissolution rates in reaction vessels (Morse et al. 1980). Since biogenic carbonates in natural systems first enter the geochemical cycle with their organic matrix and coatings intact, the protective effect of organics has implications for patterns of shell preservation during early diagenesis.

Specifically, the initial "grace period" of low mineral reactivity will generally coincide with early post-mortem seafloor exposure and shallow burial, when shells are likely to be associated with undersaturated waters. The slower the rate of microbial decomposition and the less desirable the shell to colonization by microborers, then the longer the grace period and the more likely the shell will survive residence in this diagenetic zone. The low reactivity imposed by organics can be as brief as one or two months for the most vulnerable (organic-rich) microstructures in the most aggressive (aerobic microbial undersaturated) environments. This experimental result may provide only a minimum estimate of organic protection, inasmuch as shells in other tanks showed a sharp drop in their rate of deterioration after the first 2 or 3 months (figures 4 and 7). Moreover, shells in natural settings can acquire protective post-mortem coatings (e.g., encrusting diatoms; Heinrich and Wefer 1986; Echols 1993) which can outlast or replace the original matrix, thereby prolonging the period of limited dissolution. Protective organics may thus help to explain seemingly anomalous experimental results, such as the $2\times$ slower dissolution of fresh than of bleached coccoliths observed by Keir (1980), and the $10\times$ slower rates of dissolution measured for in situ carbonate sediments than for aged material under laboratory conditions (Aller 1982; Archer et al. 1989). (Powell et al. (1990) found that some portion of a shell's original matrix might persist for hundreds to a few thousands of years post-mortem. However, the exponential curve of organic loss was calibrated using a combination of dry-stored museum specimens and extrapolation from very short-term (1–12 days) experiments on fresh shells, and so its validity for marine assemblages is uncertain.)

Another factor in the slower rates of dissolution observed for carbonates in natural systems, but not investigated here, may be the inorganic conditioning of crystallite surfaces. Organic-free biogenic aragonites in reaction vessels show very high initial rates of dissolution in undersaturated waters, matching thermodynamic values, but dissolution rates decrease rapidly over the first few weeks of reaction, presumably due to inversion of surface aragonite to a calcitic or aragonitic phase of greater chemical stability (Morse et al. 1980). Dissolution cannot resume until seawater becomes undersaturated with respect to this new surface phase. Given the similar time-scales over which organics are protective and mineral-conditioning occurs, it is possible that the two combine to lower the reactivity of fresh shell material during the first few critical months of the post-mortem period in natural systems: as organics retreat and lose their protective capability, the exposed surfaces of crystallites are shifting to more stable phases, thereby increasing the likelihood of shells forming time-averaged assemblages. In this scenario, crystallites released as particulate matter would have the highest reaction potentials owing to greatest surface area, and thus would be the primary target of dissolution. Rapid permanent burial of shells to a supersaturated zone (Aller 1982) and episodic burial during slow net sedimentation (Kidwell 1982, 1986, 1989; Davies et al. 1989) are commonly invoked preservational routes for shells and are probably operative in many settings, but even under these conditions shell accumulation would be further enhanced by lowered shell reactivities in the early post-mortem period and by the buffering effect of "sacrificial" crystallites on porewaters. Such self-buffering by shell-rich sediments has been postulated as a preservational factor in both ancient (Kidwell 1986, 1989) and modern death assemblages (Kotler et al. 1992).

High rates of dissolution in modern sediments (e.g., porewater measurements of Aller 1982 for Long Island Sound siliciclastics and of Walter and Burton 1990 for Florida Bay carbonates; calculated maximum acid-production rates of Davies et al. 1989) thus are not incompatible with the formation of long-term death assemblages of shells if, as in our experiments, dissolution is focussed preferentially on particulate matter. Our experiments

further indicate that particulate carbonate will be produced predominantly by organic-rich skeletal types, and this is consistent with some field observations. For example, although they detected 0.1 to 50% weight loss (1 yr) on pretreated implanted grains, Walter and Burton (1990) had difficulty discerning SEM evidence for dissolution on naturally occurring large shells, suggesting that dissolution had instead preferentially removed fine aragonitic mud (i.e., crystallites released by decomposition of organic-rich codiacean algae and by bioerosion) (and see preferential destruction of nacreous shells in Valentine's 1989 California siliciclastics dataset described above). Our experiments on the early post-mortem behavior of fresh shells thus complement the findings of Walter (1985) for older, organic-free grains, whose behavior is more closely ruled by mineralogy, grain size, and microstructural surface area.

Methodologically, the experiments indicate that any pretreatment that might alter or remove organic matrix deserves rigorous evaluation as a potential source of experimental artefacts. This includes not only heating and bleaching (Gaffey et al. 1991), but the use of grains that have been stored or taken from modern death assemblages rather than directly from live populations. Shells on and just below the seafloor may be hundreds to thousands of years old despite a macroscopically fresh appearance (review in Kidwell and Bosence 1991; Powell and Davies 1990; Flessa et al. 1993), and truly fresh shells experience significant loss in biomechanical strength both with drying (Westermann and Ward 1980) and with exposure to supersaturated seawater (LaBarbera and Merz 1992; Daley 1993), a phenomenon that is probably related to changes in organic matrix. Laboratory experiments on pretreated material, such as required for accurate *mineral* kinetic studies, should thus be extrapolated to natural systems with caution.

Environmental Differences. Hypothetically, organic-rich microstructures should be a greater preservational liability in some early diagenetic environments than in others. However, preservation is not a function of diagenesis alone, nor is diagenetic behavior a function of organic matrix alone, and so field-tests in modern and ancient environments will be essential.

For example, although aerated saturated and supersaturated environments are not taphonomically neutral owing to the potential for matrix loss, complete disintegration of shells requires physical reworking to dissociate loosened crystallites. If undisturbed, organic-free specimens might still be recorded as softened shells in matrix or, eventually, by molds. Environments characterized by physical reworking of sediments should thus be the most likely of saturated/supersaturated settings to show an appreciable matrix-related bias in fossil assemblages. Aerated undersaturated waters might also show a range in bias. While organic-rich microstructures should have an initial preservational advantage, this advantage would be lost with aging and matrix-loss. Bias related to mineralogy and surface area might then obliterate the trend of earlier bias.

We do not have data for anaerobic conditions, which dominate many marine porewater profiles at least seasonally (e.g., Aller 1982), but we suspect that the effects of water saturation would be similar to those observed in aerated experiments since microbial decomposition would still occur. Anaerobic rates of matrix retreat may or may not be slower than in aerobic environments: Canfield (1989) found that anaerobic rates of decomposition are slightly slower than aerobic rates for refractory organics, but Simon and Poulicek (1990) found that molluscan matrix degraded as rapidly under both conditions. The tendency of organic-rich shells to be preserved in anaerobic facies (Kennedy and Hall 1967) may thus result as much or more from those environments having experienced infrequent physical reworking than from the preservation of organic matrix.

Taxonomic Biases in Preservation. In general, taxa composed of organic-poor aragonites should be less vulnerable than those with organic-rich aragonites, and perhaps even than those with organic-rich calcites (e.g., Emig 1990; Simon et al. 1990). The presence of aragonitic taxa in a fossil assemblage thus may not ensure that all aragonitic (and calcitic) taxa present in the original community are preserved, but only those of comparable or lower (i.e., microstructurally less accessible) organic content. For example, deposit-feeding protobranch bivalves have predominantly organic-rich nacre shells whereas infaunal suspension feeding bivalves tend to have more resistant porcellaneous aragonitic microstructures, so that differential preservation could skew apparent community composition (as implied by Valentine's data, discussed above). Elevated organic content early in ontogeny (Price et al. 1976; Rosenberg 1980) may also help to explain the under-representation of juveniles in many fossil assemblages.

A larger-scale implication of matrix-related bias is that changes in the relative proportions of fossils groups over evolutionary time and the preponderance of organic-rich microstructures in "archaic" groups might lead to Phanerozoic-scale shifts in

the quality of the fossil record (Kidwell 1990). Taxa dominated by organic-rich microstructures (nacre, prismatic aragonites and prismatic calcites) are in fact commonly preserved only as molds, even when co-occurring taxa composed of organic-poor microstructures (e.g., cross-lamellar, complex cross-lamellar, and homogeneous aragonites and foliated calcite, cf. Taylor et al. 1969, 1973) are preserved with original shell material. In addition, organic-rich types rarely dominate the shell gravels that attract paleontologic attention (Kidwell 1990 and work in progress), and are prone to disintegration during collection and handling.

Conclusions. The post-mortem reactivity of biogenic carbonates is a multi-factorial system that should not be oversimplified. Bias in time-averaged sediments, for example, will not always be dominated by organic matrix even though this may be a rate-limiting factor in the early stages of diagenesis, and systematic investigation of the fossil record may well reveal environments in which high organic content consistently favors rather than undercuts skeletal preservation, for example through authigenic mineralization. However, because all biogenic skeletons are composites of minerals and organics to some degree, organic matrix and in particular its changing role during post-mortem aging certainly deserve attention comparable to that focused on the factors of mineralogy, surface area, and water chemistry.

ACKNOWLEDGMENTS

We are grateful to Munir Humayun for assistance with seawater preparation and analysis, and to Lynn M. Walter for geochemical advice and encouragement throughout in the experiment. We also thank M. LaBarbera, D. Archer, J. G. Carter, J. D. Taylor, C. A. Richardson, G. Bowie, R. J. Draus, A. M. Davis, R. Potter, D. Cameron, B. and P. Woodbury, and L. Jackson for experimental advice or assistance, and D. Archer, D. Jablonski, L. M. Walter, and three anonymous reviewers for helpful comments on the manuscript. CPG was supported by a 1990–1991 Cambridge-Chicago Undergraduate Exchange Fellowship whose donor is gratefully acknowledged. Research supported by NSF Grants EAR85-52411-PYI to SMK.

REFERENCES CITED

Alexandersson, E. T., 1975, Etch patterns on calcareous sediment grains: petrographic evidence of marine dissolution of carbonate minerals: Science, v. 189, p. 47–48.

———, 1978, Petrographic saturometry in marine carbonate sediments: Scanning Electron Microscopy, v. 1, p. 503–511.

Aller, R. C., 1982, Carbonate dissolution in nearshore terrigenous muds: the role of physical and biological reworking: Jour. Geology, v. 90, p. 79–95.

Archer, D.; Emerson, S.; and Reimers, C., 1989, Dissolution of calcite in deep sea sediments: pH and O_2 microelectrode results: Geochim. Cosmochim. Acta, v. 53, p. 2831–2845.

Canfield, D. E., 1989, Sulfate reduction and oxic respiration in marine sediments: implications for organic carbon preservation in euxinic environments: Deep-Sea Res. v. 36, p. 121–138.

Crenshaw, M. A., 1980, Mechanisms of shell formation and dissolution, *in* Rhoads, D. C., and Lutz, R. A., eds., Skeletal Growth of Aquatic Organisms: New York, Plenum Press, p. 115–132.

Currey, J. D., 1990, Biomechanics of mineralized skeletons, *in* Carter, J. G., ed., Skeletal Biomineralization: Patterns, Processes and Evolutionary Trends, Vol. 1: New York, Van Nostrand Reinhold, p. 11–25.

Daley, G. M., 1993, Passive deterioration of shelly material: a study of the Recent eastern Pacific articulate brachiopod *Terebratalia transversa* Sowerby: Palaios, v. 8, p. 226–232.

Davies, D. J.; Powell, E. N.; and Stanton, R. J., Jr., 1989, Relative rates of shell dissolution and net sediment accumulation—a commentary: can shell beds form by the gradual accumulation of biogenic debris on the sea floor?: Lethaia, v. 22, p. 207–212.

Drever, J. I., 1982, The Geochemistry of Natural Waters: Englewood Cliffs, Prentice-Hall, 388 p.

Echols, C.M.H.M.S., 1993, Diatom infestation of Recent crinoid ossicles in temperate waters, Friday Harbor Laboratories, Washington: implications for biodegradation: Palaios, v. 8, p. 278–288.

Emig, C. C., 1990, Examples of post-mortality alteration in Recent brachiopod shells and (paleo)ecological consequences: Mar. Biol., v. 104, p. 233–238.

Flessa, K. W., and Brown, T. J., 1983, Selective solution of macroinvertebrate calcareous hard parts: a laboratory study: Lethaia, v. 16, p. 193–205.

———; Cutler, A. H.,; and Meldahl, K. H., 1993, Time and taphonomy: quantitative estimates of time-averaging and stratigraphic disorder in a shallow marine habitat: Paleobiology, v. 19, p. 266–286.

Gaffey, S. J.; Kolak, J. J.; and Bronnimann, C. E., 1991, Effects of drying, heating, annealing, and roasting on carbonate skeletal material, with geochemical and diagenetic implications: Geochim. Cosmochim. Acta, v. 55, p. 1627–1640.

Garrels, R. M., and Christ, C. L., 1965, Solutions, minerals, and equilibria: New York, Harper and Row, 450 p.

Gaspard, D., 1989, Quelques aspects de la biodégradation des coquilles de brachiopodes; conséquences sur leur fossilisation: Bull. Soc. Géol. France, Sér. 8, v. 5, p. 1207–1216.

Hare, P. E., and Abelson, P. H., 1965, Amino acid composition of some calcified proteins. Carnegie Inst. Washington Yearbook, v. 64, p. 223–234.

Heinrich, R., and Wefer, G., 1986, Dissolution of biogenic carbonates: effects of skeletal structure: Mar. Geol., v. 71, p. 341–362.

Hudson, J. D., 1967, The elemental composition of the organic fraction, and the water content, of some Recent and fossil mollusc shells: Geochim. Cosmochim. Acta, v. 31, p. 2361–2378.

Jensen, M., and Thomsen, E., 1987, Ultrastructure, dissolution and "pyritization" of Late Quaternary and Recent echinoderms: Bull. Geol. Soc. Denmark, v. 36, p. 275–287.

Keir, R. S., 1980, The dissolution kinetics of biogenic calcium carbonates in seawater: Geochim. Cosmochim. Acta, v. 44, p. 241–252.

Kennedy, W. J., and Hall, A., 1967, The influence of organic matter on the preservation of aragonite in fossils: Proc. Geol. Soc. London, v. 1645, p. 325–331.

Kester, D. R.; Duedall, I. W.; Conners, D. N.; and Pytkowicz, R. M., 1967, Preparation of artificial seawater: Limnol. Ocean., v. 12, p. 176–179.

Kidwell, S. M., 1982, Time scales of fossil accumulation: patterns from Miocene benthic assemblages: Proc. Third North American Paleontol. Conv., v. 1, p. 295–300.

———, 1986, Models for fossil concentrations: paleobiological implications: Paleobiology, v. 12, p. 6–24.

———, 1989, Stratigraphic condensation of marine transgressive records: origin of major shell deposits in the Miocene of Maryland: Jour. Geology, v. 97, p. 1–24.

———, 1990, Phanerozoic evolution of macroinvertebrate shell accumulations: preliminary data from the Jurassic of Britain: Paleont. Soc. Spec. Pub., v. 5, p. 309–327.

———, and Bosence, D. W. J., 1991, Taphonomy and time-averaging of marine shelly faunas, *in* Allison, P. A., and Briggs, D. E. G., eds., Taphonomy, Releasing the Data Locked in the Fossil Record: New York, Plenum Press, p. 115–209.

Kotler, E.; Martin, R. E.; and Liddell, W. D., 1992, Experimental analysis of abrasion and dissolution resistance of modern reef-dwelling foraminifera: implications for the preservation of biogenic carbonate: Palaios, v. 7, p. 224–276.

LaBarbera, M., and Merz, R. A., 1992, Post-mortem changes in strength of gastropod shells: evolutionary implications for hermit crabs, snails, and their mutual predators: Paleobiology, v. 18, p. 367–377.

Lewy, Z., 1975, Early diagenesis of calcareous skeletons in the Baltic Sea, western Germany: Meyniana, v. 27, p. 29–33.

———, 1981, Maceration of calcareous skeletons: Sedimentology, v. 28, p. 893–895.

Lowenstam, H. A., and Weiner, S., 1989, On Biomineralization: New York, Oxford Univ. Press, 324 p.

Lutz, R. A., and Rhoads, D. C., 1977, Anaerobiosis and a theory of growth line formation: Science, v. 198, p. 1222–1227.

Mehrbach, C.; Culberson, C. H.; Hawley, J. E.; and Pytkowicz, R. M., 1973, Measurements of the apparent dissociation constants of carbonic acid in seawater at atmospheric pressure: Limnol. Oceanog., v. 18, p. 897–907.

Morse, J. W., 1986, The surface chemistry of calcium carbonate minerals in natural waters: an overview: Mar. Chem., v. 20, p. 91–112.

———; Mucci, A.; and Millero, F. J., 1980, The solubility of calcite and aragonite in seawater of 35‰ salinity at 25°C and atmospheric pressure. Geochim. Cosmochim. Acta, v. 44, p. 85–94.

Mutvei, H., 1984, Scanning electron-microscope methods: Paleont. Jour., v. 18, p. 78–82.

Paine, R. T., 1964, Ash and coloric determinations of sponge and opisthobranch tissues: Ecology, v. 45, p. 384–387.

Pilkey, O. H., and Goodell, H. G., 1964, Comparison of the composition of fossil and recent mollusk shells: Geol. Soc. America Bull., v. 75, p. 217–228.

Poulicek, M., 1983, Patterns of mollusk shell biodegradation in bathyal and abyssal sediments: Jour. Mollus. Studies, Suppl. 12A, p. 136–141.

Powell, E. N., and Davies, D. J., 1990, When is an "old" shell really old?: Jour. Geology, v. 98, p. 823–844.

———; King, J. A., and Boyles, S., 1990, Dating time-since-death of oyster shells by the rate of decomposition of the organic matrix: Archaeometry, v. 33, p. 51–68.

Price, T. J.; Thayer, G. W.; Lacroix, M. W.; and Montgomery, G. P., 1976, The organic content of shells and soft tissues of selected estuarine gastropods and pelecypods: Proc. Nat. Shellfisheries Assoc., v. 65, p. 26–31.

Rosenberg, G. D., 1980, An ontogenetic approach to the environmental significance of bivalve shell chemistry, *in* Rhoads, D. C., and Lutz, R. A., eds., Skeletal Growth of Aquatic Organisms: New York, Plenum Press, p. 133–168.

Roux, M.; Rio, M.; Schein, E.; Lutz, R. A.; Fritz, L. W.; and Ragone, L. M., 1989, Mesures in situ de la croissance des bivalves et des vestimentiféres et de la corrosion des coquilles au site hydrothermal de 13°N (dorsale du Pacifique oriental). Compt. Rendus Acad. Sci. Paris, Sér. III, v. 308, p. 121–127.

Simon, A., and Poulicek, M., 1990. Biodégradation anaérobique des structures squelettiques en milieu marin: I—approche morphologique: Cahiers Biol. Marine, v. 31, p. 95–105.

———; ———; Machiroux, R.; and Thorez, J., 1990, Bio-

dégradation anaérobique des structures squelettiques en milieu marin: II—approche chimique: Cahiers Biol. Marine, v. 31, p. 365–384.

Smith, A. M.; Nelson, C. S.; and Danaher, P. J., 1992. Dissolution behavior of bryozoan sediments: taphonomic implications for nontropical shelf carbonates: Palaeogeog. Palaeoclimat., Palaeoecol., v. 93, p. 213–226.

Taylor, J. D.; Kennedy, W. J.; and Hall, A., 1969, The shell structure and mineralogy of the Bivalvia, Introduction, Nuculacea-Trigonacea: Bull. Brit. Mus. Nat. Hist. (Zoology), Suppl. 3, 125 p.

———; ———; and ———, 1973, The shell structure and mineralogy of the Bivalvia, II. Lucinacea-Clavagellacea, conclusions: Bull Brit. Mus. Nat. Hist. (Zoology), v. 22, p. 255–294.

Turekian, K. K., and Armstrong, R. L., 1961, Chemical and mineralogical composition of fossil molluscan shells from the Fox Hills Formation, South Dakota: Geol. Soc. America Bull., v. 72, p. 1817–1828.

Valentine, J. W., 1989, How good was the fossil record? Clues from the Californian Pleistocene. Paleobiology, v. 15, p. 83–94.

Walter, L. M., 1985, Relative reactivity of skeletal carbonates during dissolution: implications for diagenesis: SEPM Spec. Pub., v. 36, p. 3–16.

———, and Burton, E. A., 1986, The effect of orthophosphate on carbonate mineral dissolution rates in seawater: Chem. Geol., v. 56, p. 313–323.

———, and ———, 1990, Dissolution of Recent platform carbonate sediments in marine pore fluids: Am. Jour. Science, v. 290, p. 601–643.

———, and Morse, J. W., 1984, Reactive surface area of skeletal carbonates during dissolution: effect of grain size: Jour. Sed. Petrol., v. 54, p. 1081–1090.

———, and ———, 1985, The dissolution kinetics of shallow marine carbonates in seawater: a laboratory study: Geochim. Cosmochim. Acta, v. 49, p. 1503–1513.

Weiss, R. F., 1974, Carbon dioxide in water and seawater, the solubility of a non-ideal gas: Marine Chem., v. 2, p. 203–215.

Westermann, G. E. G., and Ward, P. D., 1980, Septum morphology and bathymetry in cephalopods: Paleobiology, v. 6, p. 48–50.